Bio-Inspired Circular Polarized UHF RFID Tag Design using Characteristic Mode Analysis

Abubakar Sharif, Rajesh Kumar, Turke Althobaiti, Abdullah Alhumaidi Alotaibi, Lubna Safi, Naeem Ramzan, *Senior Member, IEEE*, Muhammad Ali Imran, *Senior Member, IEEE* and Qammer H. Abbasi, *Senior Member, IEEE*

***Abstract*—This paper presents a bio-inspired circularly polarized ultra-high frequency (UHF) radio frequency identification (RFID) tag antenna for metallic and low-permittivity substances. This tag design is based on a leaf-shaped radiator, two shorting stubs and slots etched on F4B substrate. Initially, the tag antenna is designed using characteristics mode analysis (CMA) by analyzing the first six CM modes and characteristic angles. The width of orthogonal slots is varied to get the resonance of CM modes in the required US RFID band. Moreover, the edges are blended to get orthogonal current distribution, which is necessary for circular polarization. Additionally, the proposed tag design is optimized further using CST Microwave studio and an RFID chip is exploited as a capacitive coupling element (CCE) to run CM modes with the orthogonal current pattern. This tag can also be tunable to European RFID (EU) band (866 – 868 MHz) by changing the length of shorter diagonal slot. The tag design offers a read range of 7 m and 4.5 m on 100 × 100 mm^2 metals plate and low-permittivity substrates, respectively (for 902 – 928 MHz band). In EU band, the corresponding read ranges are 5.7 m and 3.5 m above metal and low-permittivity objects, respectively. This circularly polarized tag antenna is advantageous in terms of cost, circular polarization feature, and ease of fabrication due to the absence of vias, shorting pins, and matching circuits. Therefore, this tag design is suitable for labeling various low-permittivity objects, industrial conveyer belt applications, baggage handling systems, and IoT applications.**

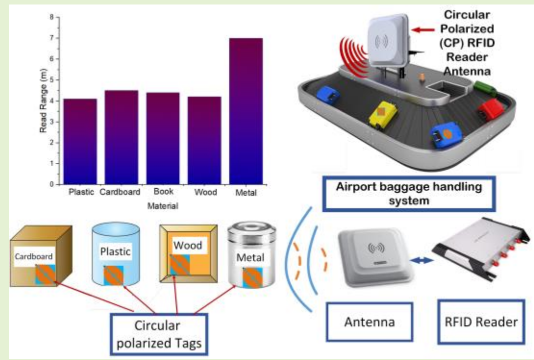

***Index Terms*— Circular polarized (CP); RFID; Tag Antenna; IoT Systems; Conveyer Belt Applications.**

I. INTRODUCTION

The authors extend their appreciation to the Deputyship for Research& Innovation, Ministry of Education in Saudi Arabia for funding this research work through the project number (IF_2020_NBU_201) and in part by the Taif University, Taif, Saudi Arabia, through the Taif University Research Grant under Project TURSP-2020/277

Abubakar Sharif and Rajesh Kumar are with Yangtze Delta Region Institute (Huzhou), University of Electronic Science and Technology of China (UESTC); rajakumarlohano@gmail.com

Abubakar Sharif is also with the Department of Electrical Engineering & Technology; Government College University Faisalabad (GCUF), Faisalabad, Pakistan; sharifuestc@gmail.com.

Turke Althobaiti is with the Department of computer science, Faculty of Science, Northern Border University, Arar, Saudi Arabia.

Turke Althobaiti is also with the Remote Sensing Unit, Northern Border University, Arar, Saudi Arabia; Turke.althobaiti@nbu.edu.sa.

Abdullah Alhumaidi Alotaibi is with the Department of Science and Technology, College of Ranyah, Taif University, P.O. Box 11099, Saudi Arabia. a.alhumaidi@tu.edu.sa.

Lubna Safi is with the Telecommunication Engineering Department, University of Engineering and Technology, Peshawar, Pakistan. Lubnaxafi@gmail.com.

Naeem Ramzan School of Computing, Engineering and Physical Sciences, University of the West of Scotland, Paisely PA12BE, UK; naeem.ramzan@uws.ac.uk.

Muhammad Ali Imran and Qammer H. Abbasi are with the James Watt School of Engineering, University of Glasgow, Glasgow G12 8QQ, U.K. (e-mail: muhammad.imran@glasgow.ac.uk.; qammer.abbasi@glasgow.ac.uk.).

INTERNET of things (IoT) and RFID have been developing concurrently, resulting in a wide variety of applications such as asset management, apparel tagging, supply chain management, air baggage handling, smart healthcare, sensing, and so forth. RFID technology has a market share of 28.4 billion tags (by tag volume) in 2021, with UHF RFID tags accounting for 23 billion tags. However, the inherited sensitivity of UHF tags to background tagging surfaces is regarded as a major impediment to their performance [1]–[7]. The performance of UHF tags is negatively impacted by surfaces like metal, the human body, and objects with high permittivity in terms of impedance mismatch and radiation efficiency [8]. Moreover, most of the commercial domain RFID systems are based on dipole-like tags, which are inheritably linear polarized. The RFID reader antennas are circular polarized (CP) to avoid misreading of LP tag antennas. However, this CP reader and LP tag combination have a polarization mismatch of 3 dB, which ultimately reduces the overall read range of RFID systems.

Muhammad Ali Imran is also with the Artificial Intelligence Research Center (AIRC), Ajman University, Ajman, UAE

* Correspondence: qammer.abbasi@glasgow.ac.uk ;

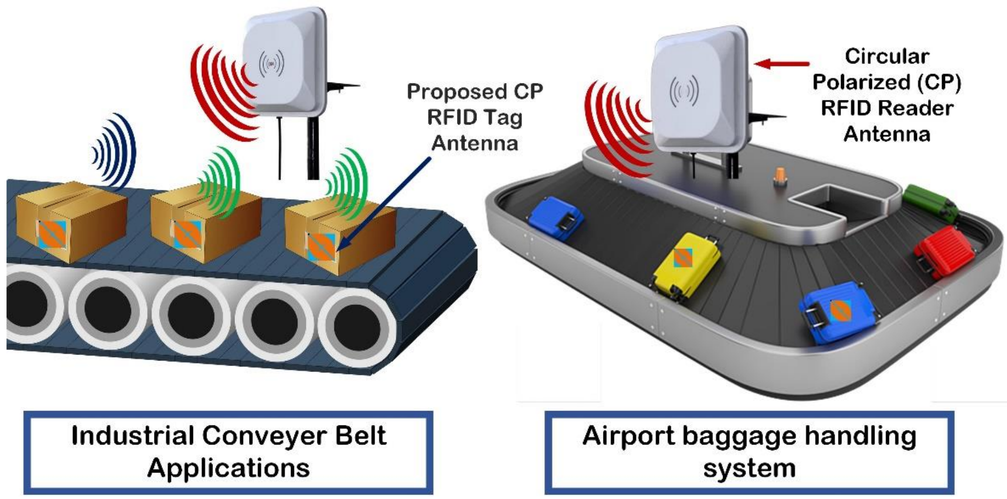

Fig. 1. Projected application areas of proposed Bio-Inspired CP tag design.

As a result, a circularly polarized RFID tag antenna is appropriate for resolving orientation issues without incurring additional loss due to polarization mismatch. There were several CP tag antennas have been reported in the literature [9], [10]. However, most of the CP tag designs were based on shorting pins, vias, and multi-layered structures, which increases the sensitivity and cost of the tag design. A corner truncated wearable RFID tag antenna based on the textile substrate was proposed in [11]. The miniaturization of the tag antenna was performed by applying a combination of cross- and L-shaped slots. Additionally, circular polarization was achieved by truncating all four corners. The size of the proposed antenna was $50 \times 50 \times 4$ mm^3. Moreover, this corner truncated CP tag antennae also has a shorting pin, which makes this tag structure costly and complex.

A CP tag antenna with optically transparent features is designed by encapsulating a thin sheet of VeilShield between two layers of flexible polydimethylsiloxane (PDMS) substrate. This tag design is based on a Square ring, meandered strip, and matching strips to achieve CP configuration and a read range of 8.3 m [12]. A circularly polarized sensor tag based on a complementary split ring resonator (CSRR) has been proposed for detecting the complex permittivity of liquids. Through a hole, the liquid under test was injected into the cavity. By adjusting the measure read range, the complex permittivity of liquids was extracted [13]. Another long-range CP tag for metallic objects has been devised in [14]. This tag utilized a two-layered substrate with a cross-slot on the top, meandered strip, and shorting line. Similarly, a planar square ring tag design has been proposed in [15] with CP features. This tag design utilized meandered strip in square ring structure to achieve a 3 dB CP bandwidth of 100 MHz in whole UHF RFID band. This tag design is fabricated on 0.2 mm thick FR4 substrates and attached to 5 mm windshield glass. The dimensions of this tag were 54×54 mm^2.

Characteristic Mode Analysis (CMA) is a systematic technique for analyzing and designing antennas and RFID tag designs [16]. A disk-shaped CP antenna has been developed for tagging metallic poles using CMA. This antenna achieved a read range of 7 m and can be readable without kneeling by exploiting the broadside radiating mode of the tag antenna using CMA [17]. A wideband CP patch antenna consists of H-shaped unit cells has been proposed in [18] using CMA. A characteristic mode analysis is performed to comprehend the various modes of a suggested antenna geometry without a feeding network. The selection of modes to create the desired radiation pattern is done by studying modal currents and their corresponding modal fields (radiation patterns). Finally, a feeding structure that will excite the desired modes and have good impedance matching is selected. As an illustration, the design procedure is used to propose and create a CP patch antenna fed with a cross-shaped aperture. The radiator is a patch made of unit cells in the shape of an H. A similar CMA based approach is used to design the proposed CP tag design.

In addition to this, many bio-inspired antenna designs have been reported in literature [19]. The symmetric structures of bio-inspired designs add both beauty and give a natural shape that can receive any kind of polarized RFID signal as the tree leafs can receive sun light with any random polarization [20], [21]. A bioinspired Linden leaf-shaped rectenna has been proposed in [22] to work on 1.6 and 2.65 GHz bands for energy harvesting applications. Similarly, a Hexa-Band Bio-inspired semi-Vine-leaf shape antenna is reported in [23]. This semi- Vine leaf shaped antenna also features asymmetric microstrip feedline Defected Ground Structure in order to achieve compactness. Another, bio-inspired Carica Papaya leaf shaped microstrip antenna was proposed in [24]. A wideband monopole bio-inspired Inga Marginata leaves shaped design has been reported in [25] for partial discharge (PD) activity detection.

A chipless RFID sensor for corrosion detection and monitoring on metallic structures has been proposed in [26]. The clipless sensor was based on frequency selective surface (FSS) and feature fusion. A simulation and experimental validation was performed to demonstrate the ability of FSS to sense and characterize corrosion thickness. Moreover, the feature fusion technique was utilized to increase reliability and sensitivity of proposed chipless sensor.

Therefore, in this paper, a bio-inspired UHF RFID tag antenna with CP and tunable characteristics is proposed for metallic and low-permittivity materials. This tag design is based on the leaf-shaped radiator, two shorting stubs and slots fabricated on F4B substrate. The first six CM modes and characteristic angles are analyzed to create the initial tag design using characteristics mode analysis. To achieve resonance of CM modes in the required US RFID band, the width of the orthogonal slots is varied.

Additionally, the edges are curved to obtain the orthogonal current distribution required for circular polarization. By adjusting the length of the shorter diagonal slot, this tag can also be tuned to the European RFID band (866 - 868 MHz). In the EU band, the corresponding read ranges are 5.7 m and 3.5 m above metal and low-permittivity objects, respectively.

Furthermore, an RFID chip is used as a capacitive coupling element (CCE) to run CM modes with an orthogonal current pattern, and the suggested tag design is further optimized using CST Microwave Studio. The tag design offers a read range of 7 m and 4.5 m on 100 × 100 mm^2 metal plates and low-permittivity substrates, respectively. Consequently, this tag design is suitable for labeling metallic objects, industrial conveyer belt applications, and baggage handling systems as illustrated in Fig. 1.

II. Antenna Concept and Design

Fig. 2 illustrates the detailed dimensions and geometry of the proposed CP tag antenna for both 915 MHz and 866 MHz. This tag design consists of a bio-inspired rosewood tree leaf-shaped radiator, two orthogonal slots fabricated on a 2 mm thick grounded F4B substrate (F4B is low cost as compared to Rogers substrate with dielectric constant 3.28 and the dielectric loss tangent 0.001.

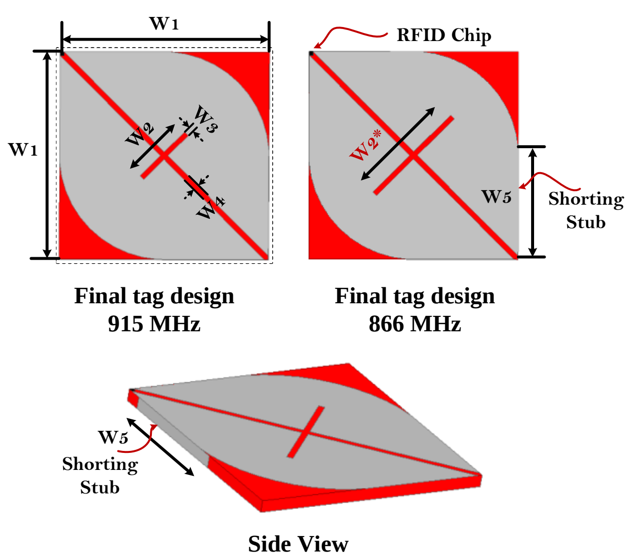

Fig. 2. Geometry and Detailed dimensions proposed CP tag design (W_1= 40 mm, W_2= 16 mm, W_2^*= 21 mm, W_3= 1 mm, W_4= 1.05 mm, W_5= 23.5 mm, h_1= 2 mm).

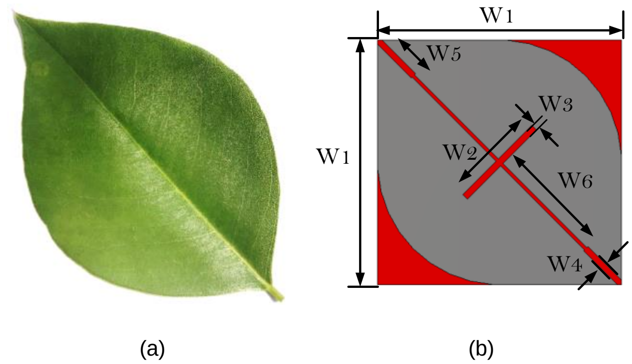

Fig. 3. (a) Rosewood tree leaf (b) Detailed dimensions of initial tag design (W_1=40 mm, W_2=16 mm, W_3=0.5 mm, W_4=0.5 mm, W_5=7.8 mm, W_6=19.5 mm, h_1=2 mm).

F4B is high frequency material based on Polytetrafluoroethylene (PTFE) glass fiber cloth and ceramic-filled PTFE glass fiber cloth. It is a kind of thermoplastic material renowned for its strong mechanical qualities, high temperature endurance, and good electrical insulation qualities.). Moreover, there are also two shorting stubs, that are connected to the ground plane at diagonally opposite ends of the leaf-shaped radiator as depicted in Fig. 2. The Alien H3 RFID chip is connected at one end of a long diagonal slot for getting a conjugate impedance match with 27 – 201j at 915 MHz. All other dimensions for 866 MHz band tag are same except the length of shorter diagonal slot.

Starting with CMA of a 40 × 40 mm^2 radiating plate etched on grounded F4B substrate, we discovered some modes are resonating near 2 and 3 GHz. In order to reduce the resonance frequency of CM modes in the US RFID band, the longer diagonal slot was designed. Additionally, the rosewood leaf (as shown in figure 3 (a)) was the bio inspiration for this proposed CP tag antenna. Thereby, an edge truncation and a small diagonal slot were carried out in order to achieve circular polarization.

Fig. 3 illustrates the initial design of the proposed tag antenna using CMA, before optimization and full wave simulation. All dimensions of the initial tag design are the same as the final proposed design except the length and width of the longer diagonal slot. The diagonal slot is 0.25 mm for W_6 portion and 0.5 mm for W_5 portion. The initial design represented in Fig. 3 is used to rum CM Analysis. Fig. 4 (a) depicts the modal significance plot of six modes of initial tag design (ITD). It can be observed that modes 1 and 2 are the most significant or resonating modes. Modes 1 and 2 are resonating at 940 MHz and 870 MHz, respectively. So, modes 1 and 2 have good radiation capability and can be excited carefully to work in the US RFID band. While modes 3, 4, 5 and 6 have modal significance less than 0.2, that demonstrates their less radiation capability. Consequently, all other modes except modes 1 and 2 are non-significant modes and cannot be excited for RFID band. Similarly, the characteristic angles of six characteristic modes (CMs) of ITD are depicted in Fig. 4 (b).

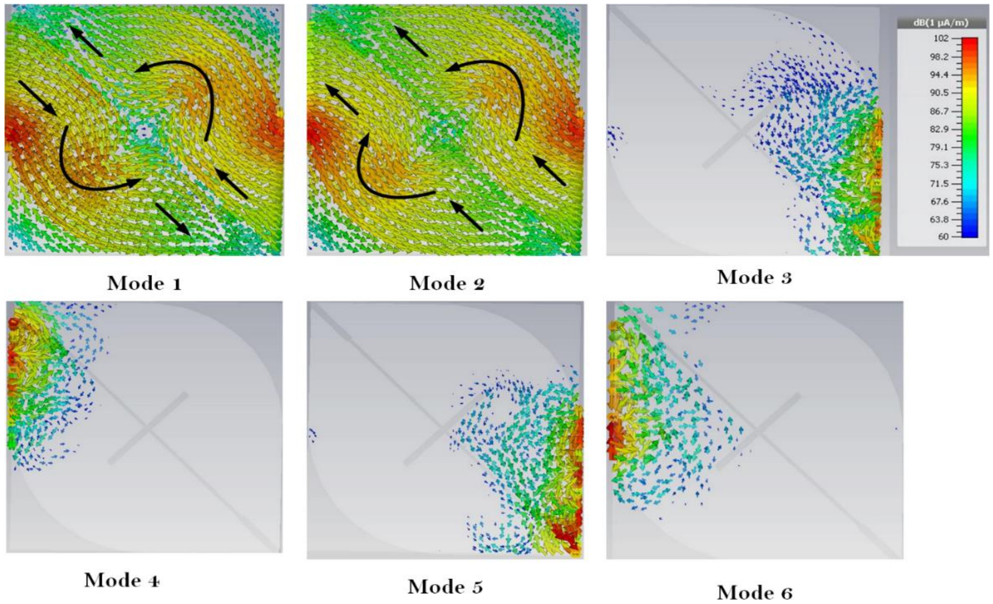

Fig. 5. Characteristics current patterns associated with six CM modes of ITD.

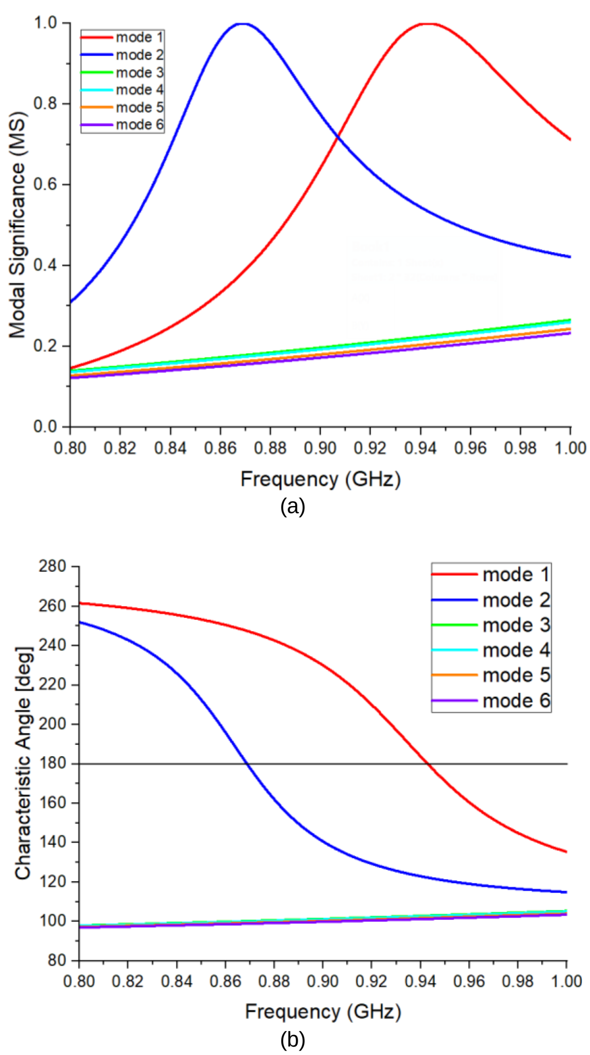

Fig. 4. (a) Modal significance of first six modes of initial tag design (b) Characteristic angles (in degrees) associated with first six modes of initial tag design.

The parameters such as modal significance (MS) and characteristic angle (α) can be extracted from eigen values λ. Both modal significance and characteristic angle are independent of source or excitation. Based on orthogonality of Characteristic modes, the overall current on perfectly electrically conducting (PEC) body or can be described as a linear superposition of characteristic mode currents as follows:

$$\vec{J} = \sum_n \alpha_n \vec{J}_n \tag{1}$$

Where $\vec{J}_n$ is eigen current or eigen function of mode n. α_n is the complex modal weighting coefficient (MWC) of mode n. MWC determines the weight or contribution of each individual mode in total current.

α_n can be expressed as:

$$\alpha_n = \frac{V_n^i}{1+\lambda_n} = \frac{\left\langle E^i, J_n \right\rangle}{1+\lambda_n} \tag{2}$$

Where V_n^i is model excitation coefficient (MEC).

Moreover, the total current $\vec{J}$ can also be described as follow:

$$\vec{J} = \sum_n \frac{V_n^i \vec{J}_n}{1+\lambda_n} \tag{3}$$

The product $V_n^i \vec{J}_n$ provide the information regarding which mode will be excited with external feed or excitation (E^i).

Moreover, the total far-fields associated with total induced currents $\vec{J}$ of can also be determined as follows [27],[28]:

$$E = \sum_n \alpha_n E_n \qquad H = \sum_n \alpha_n H_n \tag{4}$$

Where E_n and H_n are radiation far-fields associated with particular characteristic mode current n.

The characteristics angle is another important parameter to describe the exact resonance frequency of CMs. Moreover, the characteristic angles also provide significant information to achieve circular polarization. Characteristic angle (α_n) poses another important description of CMs [27] expressed as follow:

$$\alpha_n = 180 - \tan^{-1}\lambda_n \tag{5}$$

Where λn is eigenvalues associated with each CM.

The characteristics angles are very important to finding the feeding position to excite two orthogonal modes for achieving circular polarization. More precisely, in order to achieve circular polarization, two modes having a characteristic angle difference of 90º are required to excite simultaneously using one feed location [27] [28]. As it can be seen from Fig. 4 (b), the difference in characteristics angle of modes 1 and 2 at 920 MHz is 90º, which is pivotal for circular polarization. Additionally, the characteristic angles of all other modes (Modes 3, 4, 5, and 6) are between 90º to 180º, thereby posing. inductive behavior.

To explore it further, the characteristic current patterns associated with all six CM modes of ITD are shown in Fig. 5. The characteristic currents are also evident regarding the significance and radiation capabilities of modes 1 and 2. Mode 1 has a rotational current pattern with minima at the edge of a longer diagonal slot. While mode 2 also has a diagonally symmetric current pattern with minima at the edges of diagonal slots as well. The characteristic current patterns of all other modes (except modes 1 and 2) show no evident current distributions, accordingly representing the inductive behavior of these modes (modes 3 - 6). Additionally, the current distribution offers de-tails regarding the feed position to simultaneously excite both modes with an orthogonal current distribution to realize circular polarization.

III. Simulation and Measured Results

After placing the RFID chip as CCE at one end of a longer diagonal slot, modes 1 and 2 are excited. The overall tag setup is run using full-wave simulation in CST Microwave Studio (frequency domain solver) by attaching a mimic of the Alien H3 RFID chip. The width of the diagonal slot is optimized further using full-wave simulation in order to get a good impedance match with the Alien H3 RFID chip. The width of the longer diagonal slot is made 1.05 mm wide for the whole length in contrast to IDT (as shown in Fig. 2). Consequently, the resulted real and imaginary impedance plots of the proposed CP tag design (after placing over a 100 × 100 mm^2 metal plate) are shown in Fig. 6.

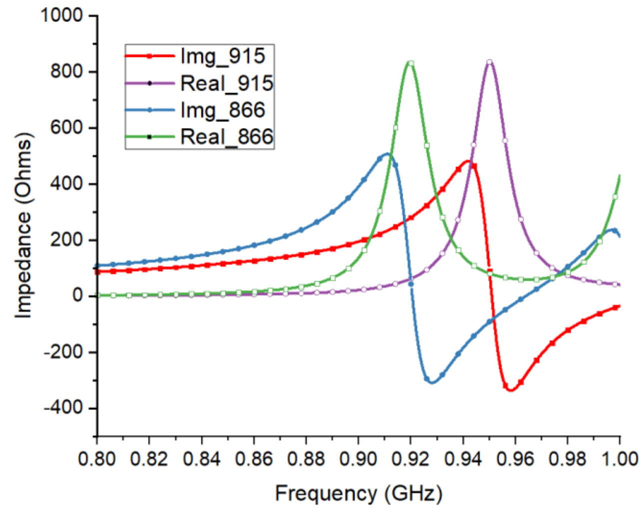

Fig. 6. Real and Imaginary impedance plot of the proposed CP tag design.

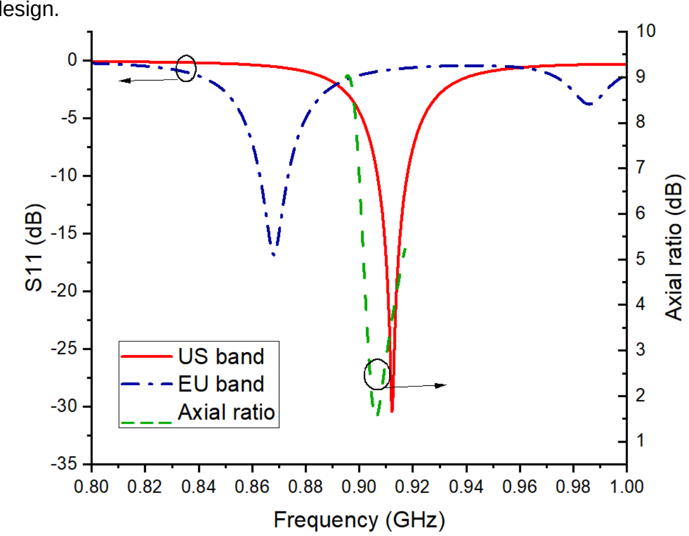

Fig. 7. Simulated S11 and axial ratio plot of proposed CP tag design.

The imaginary impedance of the CP tag ranges from 190 – 250 Ω in US RFID band (902 – 928 MHz). Similarly, the real impedance of CP design also ranges from 25 – 50 Ω in US RFID band. So, these impedance ranges of CP tag design depict a good conjugate match with H3 RFID chip having impedance 27-201j at 915 MHz. Similarly, the imaginary impedance of tag version for 866 MHz is ranging from 180 – 240 Ω. While, the real impedance in 866 MHz band is ranging from 22 – 45 Ω. So, the tunable version of this CP tag also provides good conjugate match with H3 chip in EU RFID band. The corresponding simulated S11 plot of the proposed CP tag design for both 915 MHz and 866 MHz bands are shown in Fig. 7. The 3dB band-width of this CP tag is ranging from 890 - 935 MHz, while the proposed CP design features –10 dB reflection coefficient bandwidth ranging from 900 – 920 MHz. Moreover, the axial ratio of the proposed CP tag is also shown in Fig. 7. This CP tag offers an axial ratio less than 3 dB for the 902 – 912 MHz.

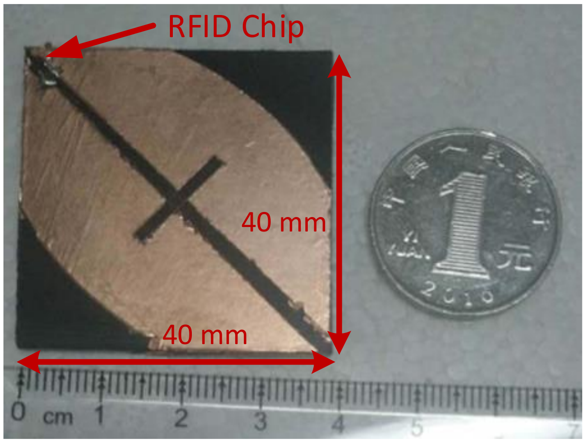

Fig. 8. Fabricated prototype of proposed CP tag design.

Fig. 8 shows a fabricated prototype of the proposed CP tag. This fabricated tag design is used for read range measurement proposes. The theoretical read range of an RFID tag can be calculated from Frii's equation as follows:

$$r_{max} = \frac{\lambda}{4\pi}\sqrt{\frac{P_{tr}G_{tr}G_{tag}(1-|\Gamma|^2)\rho}{P_{th}}} \quad (2)$$

Where λ is the wavelength, P_{tr} and G_{tr} are transmitted power of reader and reader antenna gain. G_{tag} and P_{th} are gain and minimum threshold power to turn on the tag's chip. As per datasheet [29], P_{th} of Alien H3 RFID chip is -18 dBm. Γ and ρ are reflection coefficient and polarization efficiency for the tag. The reflection coefficient accounts for impedance match, while polarization efficiency accounts for polarization mismatch (e.g. there is a 3 dB mismatch between linear polarized tag and CP reader antenna). However, there is no loss due to polarization mismatch in the case of our proposed CP tag antenna.

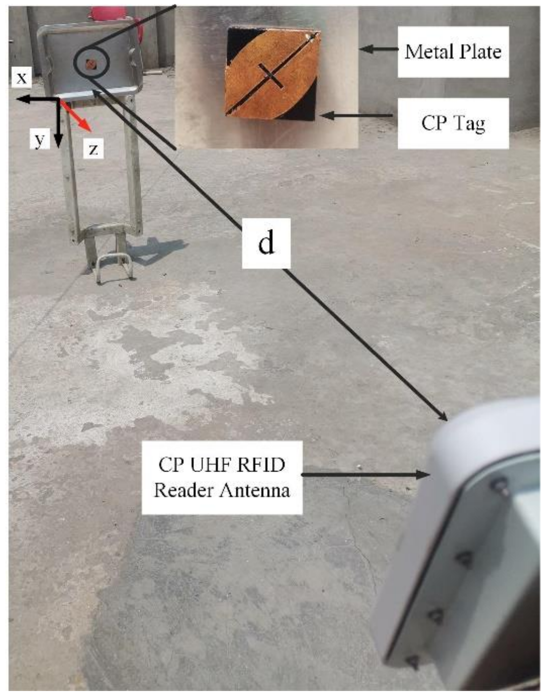

Fig. 9. Read range measurement setup for proposed CP tag after mounting on metal plate.

To conduct the read range measurements of proposed CP tag, an Impinj Speedway R420 is deployed with 8 dBi circular polarized read antenna. The outfield read range measurement setup is shown in Fig. 9. We used a frequency range of 902 – 928 MHz with 36 dBm EIRP (4 watts) specifications for reading range estimation.

Table I shows the comparison of the proposed circular polarized RFID tag with state of the art designs reported in literature. Most of the CP tags are based on single layer substrate and lack the metal tolerable feature such as reported in [9]-[13].

TABLE I
COMPARISON OF THE PROPOSED CP TAG ANTENNA WITH OTHERS DESIGNS IN THE LITERATURE

Reference	Size (mm^3)	Substrate Layers	-10 dB Impedance Bandwidth (MHz)	Maximum Read Range on Metals (m)	Maximum Read Range on other materials (m)	Via or shorting Pin	Metal Tolerant	Tunable
[9]	35.6 × 35.6 × 0.508	1	37	N.A.	7.6 (air)	No	No	No
[10]	90 × 90 mm^2	1	52	N.A.	16.3 (air)	No	No	No
[11]	50 × 50 × 4	2	N.A	N.A.	5.8 (human body)	Yes	No	No
[12]	69 × 69 × 1	2	47	N.A.	8.3 (air)	No	No	No
[13]	65 × 65 × 4	1	NA	NA	1.97	No	NA	NA
[14]	60 × 60 × 3.084	2	8	22.4	N.A.	Yes	Yes	No
[15]	54 × 54 × 5.2	2	36 (3dB)	N.A.	8.3 (air)	No	No	No
[30]	56 × 56 × 0.4	1	865.6–1000	N.A.	9.9 (air)	No	No	No
This Work	40 × 40 × 2	1	20	7	4.5	No	Yes	Yes

N.A. = Not Available, NA= Not Applicable

The tag design published in [14] was based on dual substrate layer. This design offers good read range and metal tolerable feature. However, this design offers a very small impedance bandwidth of 8 MHz and has shorting pin, which poses difficulties in tag fabrication process. The tag presented in [15] is also based on double substrate layer and has read range of 8.3 m in air. Similarly, the tag design presented in [29] is single layer structure with good impedance bandwidth and read range of 9.9 m in air. However, this tag design lacks metal tolerability and tunable features.

Therefore, the proposed tag design is good candidate among CP design with relatively small foot print of 40 × 40 × 2 mm^3. Moreover, the proposed design features read range of 7 m and 4.5 m on 100 × 100 mm^2 metals plate and low-permittivity substrates, respectively (for 902 – 928 MHz band). In EU band, the corresponding read ranges are 5.7 m and 3.5 m above metal and low-permittivity objects, respectively. This circularly polarized tag antenna is advantageous in terms of cost, circular polarization feature, and ease of fabrication due to the absence of vias, shorting pins, and matching circuits.

Since the antenna used in this setup has a gain of 8 dBi, so, the 28 dBm power specification was selected in reader setup. The read range patterns of this CP tag after mounting on metal plate and cardboard box (at 915 MHz) are illustrated in Figure 10. A read range of 7 m is achieved for both xz- and yz-planes with a maximum read range at 90° (or when the tag is face to face with the reader antenna). Similarly, this tag antenna achieved a maximum read range of 4.5 m after mounting on cardboard box for both xz- and yz-planes with a maximum read range at 90°. The read range patterns are similar with little difference in case of cardboard. Moreover, the read range in case of metal is more as compared to read range on cardboard box.

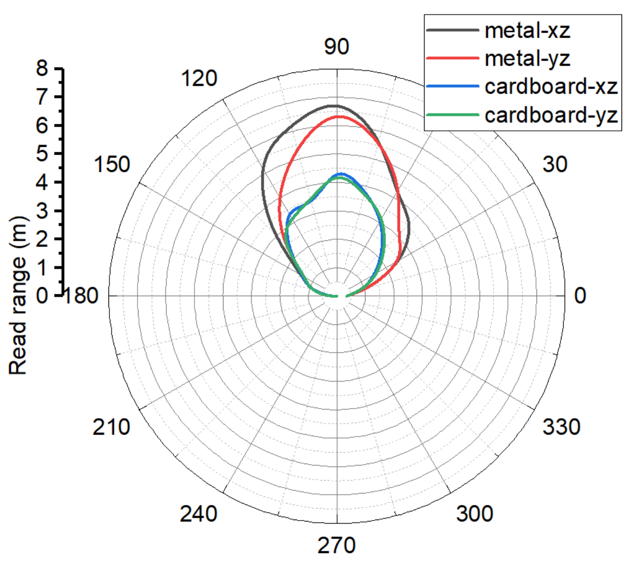

Fig. 10. Read range pattern of proposed CP tag after mounting on the metal plate.

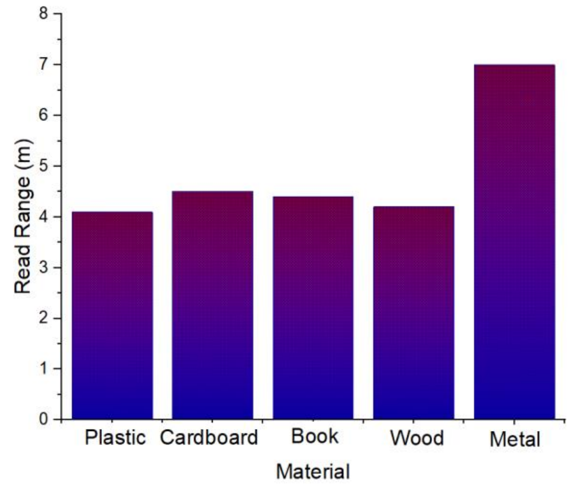

Fig. 11. Read range of proposed CP tag after mounting on different materials.

Furthermore, the tag antenna is mounted on different materials such as plastic, cardboard box, book, wooden block and 100 × 100 mm^2 metal plate. The measured read range of CP tag antenna after mounting on different materials is depicted in Figure 11. The maximum read range of 7 m is achieved on 100 × 100 mm^2 metal plate, while the read ranges achieved on plastic, book, cardboard box and wooden block are approximately 4.5 m.

In addition, by merely adjusting the length of the shorter diagonal slot, the CP tag can be tuned to the European RFID band (866 - 868 MHz). In the EU band, the corresponding read ranges are 5.7 m and 3.5 m above metal and low-permittivity objects, respectively. Therefore, the proposed CP tag antenna is a suitable candidate for tagging cardboard boxes for conveyer belt applications and baggage sorting areas at airports and other facilities.

IV. Conclusion

We propose a bio-inspired UHF RFID tag antenna with CP and tunable characteristics for metallic and low-permittivity substances. The tag parameters are optimized first using CMA to scale down the frequency of the tag in 902 – 928 MHz band. Moreover, this tag design achieved a good impedance match with the Alien H3 RFID chip after further modification using CST. The proposed CP tag attained a read range of 7 m and 4.5 m on the metal plate and low-permittivity substances. In addition, the CP tag is tunable to European RFID (EU) band (866 – 868 MHz) by just changing the length of shorter diagonal slot and obtained a corresponding read range of 5. 7 m and 3.5 m above metal and low-permittivity objects in EU band. This circularly polarized tag antenna is advantageous in terms of cost, circular polarization features, and ease of fabrication due to the absence of vias, shorting pins, and any other matching circuits. Therefore, this tag design is suitable for labeling metallic objects, industrial conveyer belt applications, baggage handling systems, and IoT applications. Future work might include combining this tag design along with suitable reader antenna for tracking and tracing of medical assets in a hospital environment.

References

[1] E. Perret, S. Tedjini, and R. S. Nair, “Design of antennas for UHF RFID tags,” Proc. IEEE, vol. 100, no. 7, pp. 2330–2340, 2012, doi: 10.1109/JPROC.2012.2186950.

[2] A. Sharif et al., “Low-cost inkjet-printed UHF RFID tag-based system for internet of things applications using characteristic modes,” IEEE Internet Things J., vol. 6, no. 2, pp. 3962–3975, Apr. 2019, doi: 10.1109/JIOT.2019.2893677.

[3] R. Abdulghafor et al., “Recent Advances in Passive UHF-RFID Tag Antenna Design for Improved Read Range in Product Packaging Applications: A Comprehensive Review,” IEEE Access, vol. 9, pp. 63611–63635, 2021, doi: 10.1109/ACCESS.2021.3074339.

[4] C. Occhiuzzi et al., “Radio-frequency-identification-based intelligent packaging: Electromagnetic classification of tropical fruit ripening,” IEEE Antennas Propag. Mag., vol. 62, no. 5, pp. 64–75, Oct. 2020, doi: 10.1109/MAP.2020.3003212.

[5] P. Escobedo, M. A. Carvajal, L. F. Capitán-Vallvey, J. Fernández-Salmerón, A. Martínez-Olmos, and A. J. Palma, “Passive UHF RFID tag for multispectral assessment,” Sensors (Switzerland), vol. 16, no. 7, p. 1085, Jul. 2016, doi: 10.3390/s16071085.

[6] F. Costa, S. Genovesi, M. Borgese, A. Michel, F. A. Dicandia, and G. Manara, “A review of rfid sensors, the new frontier of internet of things,” Sensors, vol. 21, no. 9, 2021, doi: 10.3390/s21093138.

[7] A. Sharif, J. Ouyang, A. Raza, M. A. Imran, and Q. H. Abbasi, “Inkjet-printed UHF RFID tag based system for salinity and sugar detection,” Microw. Opt. Technol. Lett., vol. 61, no. 9, pp. 2161–2168, 2019, doi: 10.1002/mop.31863.

[8] F. Erman et al., “Miniature compact folded dipole for metal mountable UHF RFID tag antenna,” Electron., vol. 8, no. 6, p. 713, Jun. 2019, doi: 10.3390/electronics8060713.

[9] H. H. Tran, S. X. Ta, and I. Park, “A Compact Circularly Polarized Crossed-Dipole Antenna for an RFID Tag,” IEEE Antennas Wirel. Propag. Lett., vol. 14, pp. 674–677, 2015, doi: 10.1109/LAWP.2014.2376945.

[10] H. D. Chen, C. H. Tsai, C. Y. D. Sim, and C. Y. Kuo, “Circularly polarized loop tag antenna for long reading range RFID applications,” IEEE Antennas Wirel. Propag. Lett., vol. 12, pp. 1460–1463, 2013, doi: 10.1109/LAWP.2013.2288138.

[11] D. Le, S. Ahmed, L. Ukkonen, and T. Bjorninen, “A Small All-Corners-Truncated Circularly Polarized Microstrip Patch Antenna on Textile Substrate for Wearable Passive UHF RFID Tags,” IEEE J. Radio Freq. Identif., vol. 5, no. 2, pp. 106–112, Jun. 2021, doi: 10.1109/JRFID.2021.3073457.

[12] A. S. M. Sayem et al., “Optically Transparent Flexible Robust Circularly Polarized Antenna for UHF RFID Tags,” IEEE Antennas Wirel. Propag. Lett., vol. 19, no. 12, pp. 2334–2338, Dec. 2020, doi: 10.1109/LAWP.2020.3032687.

[13] Y. Chen, C. Hua, and Z. Shen, “Circularly Polarized UHF RFID Tag Antenna for Wireless Sensing of Complex Permittivity of Liquids,” IEEE Sens. J., vol. 21, no. 23, pp. 26746–26754, Dec. 2021, doi: 10.1109/JSEN.2021.3121714.

[14] P. Wang, W. Luo, Y. Shao, and H. Jin, “An UHF RFID Circularly Polarized Tag Antenna with Long Read Distance for Metal Objects,” IEEE Antennas Wirel. Propag. Lett., vol. 21, no. 2, pp. 217–221, 2022, doi: 10.1109/LAWP.2021.3122871.

[15] J. H. Lu and B. S. Chang, “Planar Compact Square-Ring Tag Antenna with Circular Polarization for UHF RFID Applications,” IEEE Trans. Antennas Propag., vol. 65, no. 2, pp. 432–441, 2017, doi: 10.1109/TAP.2016.2633162.

[16] J. J. Adams, S. Genovesi, B. Yang, and E. Antonino-Daviu, “Antenna Element Design Using Characteristic Mode Analysis: Insights and research directions,” IEEE Antennas Propag. Mag., vol. 64, no. 2, pp. 32–40, Apr. 2022, doi: 10.1109/MAP.2022.3145718.

[17] Y. Yan, J. Ouyang, X. Ma, R. Wang, and A. Sharif, “Circularly Polarized RFID Tag Antenna Design for Metallic Poles Using Characteristic Mode Analysis,” IEEE Antennas Wirel. Propag. Lett., vol. 18, no. 7, pp. 1327–1331, 2019, doi: 10.1109/LAWP.2019.2915369.

[18] C. Zhao and C. F. Wang, “Characteristic Mode Design of Wide Band Circularly Polarized Patch Antenna Consisting of H-Shaped Unit Cells,” IEEE Access, vol. 6, no. Cm, pp. 25292–25299, 2018, doi: 10.1109/ACCESS.2018.2828878.

[19] A. J. R. Serres et al., “Bio-Inspired Microstrip Antenna,” in Trends in Research on Microstrip Antennas, IntechOpen, 2017.

[20] “Research Part 2: Leaf Margin Analysis | UWyo Dioramas.” https://uwyodioramas.wordpress.com/2013/02/26/research-and-leaf-margin-analysis/ (accessed Dec. 10, 2022).

[21] P. P. Shibayev and R. G. Pergolizzi, “The Effect of Circularly Polarized light on the growth of plants,” Int. J. Bot., vol. 7, no. 1, pp. 113–117, 2011, doi: 10.3923/ijb.2011.113.117.

[22] K. Çelik and E. Kurt, “Design and implementation of a dual band bioinspired leaf rectenna for RF energy harvesting applications,” Int. J. RF Microw. Comput. Eng., vol. 31, no. 11, p. e22868, Nov. 2021, doi: 10.1002/mmce.22868.

[23] J. O. Abolade, D. B. O. Konditi, and V. M. Dharmadhikary, “Compact hexa-band bio-inspired antenna using asymmetric microstrip feeding technique for wireless applications,” Heliyon, vol. 7, no. 2, p. e06247, Feb. 2021, doi: 10.1016/j.heliyon. 2021.e06247.

[24] J. O. Abolade, D. B. O. Konditi, and V. M. Dharmadhikary, “Bio-inspired wideband antenna for wireless applications based on perturbation technique,” Heliyon, vol. 6, no. 7, p. e04282, Jul. 2020, doi: 10.1016/j.heliyon. 2020.e04282.

[25] J. Do Nascimento Cruz *et al.*, “Bio-inspired printed monopole antenna applied to partial discharge detection,” *Sensors (Switzerland)*, vol. 19, no. 3, p. 628, Feb. 2019, doi: 10.3390/s19030628.

[26] A. M. J. Marindra and G. Y. Tian, “Chipless RFID sensor for corrosion characterization based on frequency selective surface and feature fusion,” Smart Mater. Struct., vol. 29, no. 12, p. 125010, Oct. 2020, doi: 10.1088/1361-665X/abbff4.

[27] M. Cabedo-Fabres, E. Antonino-Daviu, A. Valero-Nogueira, and M. F. Bataller, “The theory of characteristic modes revisited: A contribution to the design of antennas for modern applications,” IEEE Antennas Propag. Mag., vol. 49, no. 5, pp. 52–68, 2007, doi: 10.1109/MAP.2007.4395295.

[28] Y. Chen and C. F. Wang, Characteristic Modes: Theory and Applications in Antenna Engineering. 2015.

[29] “Higgs® 3 | Alien Technology.” https://www.alientechnology.com/products/ic/higgs-3/ (accessed Feb. 10, 2023).

[30] D. Inserra and G. Wen, “Compact Crossed Dipole Antenna with Meandered Series Power Divider for UHF RFID Tag and Handheld Reader Devices,” IEEE Trans. Antennas Propag., vol. 67, no. 6, pp. 4195–4199, Jun. 2019, doi: 10.1109/TAP.2019.2905926.

Abubakar Sharif received the M.Sc. degree in electrical engineering from the University of Engineering and Technology, Lahore, Pakistan, and the Ph.D. degree in electronics engineering from the University of Electronic Science and Technology of China (UESTC). From 2011 to 2016, he worked as a Lecturer with Government College University Faisalabad (GCUF), Pakistan. He is also working as a Research Fellow with UESTC. He is the author of several peer-reviewed international journal and conference papers. His research interests include wearable and flexible sensors, compact antenna design, antenna interaction with the human body, antenna and system design for RFID, phased array antennas, passive wireless sensing, and the Internet of Things (IoTs).

Muhammad A. Imran (SM 12) received the M.Sc. (Hons.) and Ph.D. degrees from Imperial College London, U.K., in 2002 and 2007, respectively. He is Dean University of Glasgow UESTC and a Professor of communication systems with the James Watt School of Engineering, University of Glasgow. He is an Affiliate Professor at the University of Oklahoma, USA, and a Visiting Professor at the 5G Innovation Centre, University of Surrey, U.K. He is leading research in University of Glasgow for Scotland 5G Center. He has over 18 years of combined academic and industry experience, working primarily in the research areas of cellular communication systems. He has been awarded 15 patents, has authored/co-authored over 500 journal and conference publications, and has been principal/coprincipal investigator on over £8 million in sponsored research grants and contracts. He has supervised 40+ successful Ph.D. graduates. He has an award of excellence in recognition of his academic achievements, conferred by the President of Pakistan. He was also awarded the IEEE Comsoc's Fred Ellersick Award 2014, the FEPS Learning and Teaching Award 2014, and the Sentinel of Science Award 2016. He is a shortlisted finalist for The Wharton-QS Stars Awards 2014, the QS Stars Reimagine Education Award 2016 for innovative teaching, and VC's Learning and Teaching Award from the University of Surrey. He is a Senior Fellow of the Higher Education Academy, U.K. He is the editor/co-editor of 8 books.

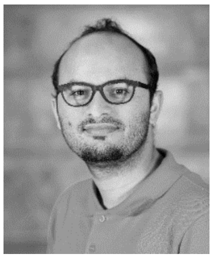

Qammer H. Abbasi (Senior Member, IEEE) is currently a Reader with the James Watt School of Engineering, University of Glasgow, Glasgow, U.K., and the Deputy Head for Communication Sensing and Imaging Group. He has authored or coauthored more than 350 leading international technical journal and peer reviewed conference papers and ten books. He was the recipient of several recognitions for his research, including URSI 2019 Young Scientist Awards, U.K. exceptional talent endorsement by Royal Academy of Engineering, Sensor 2021 Young Scientist Award, National talent pool award by Pakistan, International Young Scientist Award by NSFC China, National interest waiver by USA and eight best paper awards. He is a ommittee Member of IEEE APS Young professional, Sub-committee Chair of IEEE YP Ambassador program, IEEE 1906.1.1 standard on nano communication, IEEE APS/SC WG P145, IET Antenna & Propagation, and healthcare network. He is also a member of IET and a Fellow of RET and RSA.